

On the use of mulching to mitigate permafrost thaw due to linear disturbances in sub-arctic peatlands



Aaron A. Mohammed^{a,*}, Robert A. Schincariol^a, William L. Quinton^b, Ranjeet M. Nagare^c, Gerald N. Flerchinger^d

^a Department of Earth Sciences, University of Western Ontario, 1151 Richmond Street N, London, ON N6A 5B7, Canada

^b Cold Regions Research Centre, Wilfrid Laurier University, 75 Avenue West, Waterloo, ON N2L 3C5, Canada

^c Water Business Unit, WorleyParsons Canada, 4445 Calgary Trail, Edmonton, AB T6H 5R7, Canada

^d USDA Agricultural Research Service, Northwest Watershed Research Center, 800 Park Boulevard, Suite 105, Boise, ID 83712, USA

ARTICLE INFO

Article history:

Received 3 March 2016

Received in revised form 1 February 2017

Accepted 18 February 2017

Keywords:

Linear disturbance
Heat and water movement
Permafrost
Peat
Climate chamber
Ecohydrology

ABSTRACT

The presence or absence of permafrost strongly influences the hydrology and ecology of northern watersheds. Resource exploration activities are currently having profound effects on hydrological and ecological processes in sub-arctic peatlands. In wetland-dominated zones of discontinuous permafrost, permafrost occurs below tree-covered peat plateaus where the tree-canopy and vadose zone act to insulate and preserve permafrost below. Linear disturbances such as seismic lines result in removal of the canopy, and cause permafrost thaw, which results in increased soil moisture, land subsidence, and deforestation. This contributes to land-cover transformation, habitat and vegetation loss, and changes to basin hydrologic cycles. The resultant permafrost-degraded corridors comprise large portions of the drainage density of sub-arctic basins, and alter the region's water and energy balances. Mulching over disturbances, with the removed tree canopy, has been proposed as a best management practice to help reduce this environmental impact. Here we present climate chamber and numerical modeling results which quantify the effects of mulching and its ability to limit permafrost thaw and alterations to the ground thermal regime. Overall, the thermal buffering ability of the mulch had beneficial effects on slowing thaw, due to its low thermal conductivity, which decouples the subsurface from meteorological forcing and impedes heat conduction. Results indicate that mulching is an effective technique to reduce permafrost thaw and provides a scientific basis to assess the mitigation measure on its ability to slow permafrost degradation. This study will provide guidance as to how northern exploration may be performed in a more environmentally sustainable manner.

© 2017 Elsevier B.V. All rights reserved.

1. Introduction

Hydrological and ecological processes in northern latitudes are strongly coupled and influenced by the distribution of permafrost and peatlands (Woo and Winter, 1993). When present, the spatial characteristics of permafrost controls watershed hydrology by creating barriers and channels in the subsurface, directing water movement during summer months and modulating the ground's temperatures and energy balance (Woo, 1986). Peatlands cover

approximately 12% of Canada's land surface (Tarnocai, 2006), of which approximately 30% is underlain by permafrost (Aylsworth et al., 1993; Zoltai, 1993). Exploration practices resulting in tree canopy removal have led to widespread permafrost degradation in northern peatlands (Quinton et al., 2009; Williams et al., 2013). Linear disturbances are increasing occurrences in northern Canada; pipelines, winter roads and seismic lines now account for large portions of the drainage density of watersheds in the Canadian sub-arctic (Quinton et al., 2011). The most common types of linear disturbances are seismic lines, created during oil and gas exploration. In the zone of discontinuous permafrost, these disturbances have led to a suite of environmental impacts on the hydrologic and ecological functioning of these sensitive ecosystems. Impacts include changes in the basin hydrology, vegetation growth, habitat destruction and entire land-cover change, including permafrost thaw, ground surface subsidence, and inundation (Beilman and

* Corresponding author. Current address: Department of Geoscience, University of Calgary, 2500 University Drive NW, Calgary, AB T2N 1N4, Canada.

E-mail addresses: amohamme@ucalgary.ca (A.A. Mohammed), schincar@uwo.ca (R.A. Schincariol), wquinton@wlu.ca (W.L. Quinton), ranjeet.nagare@worleyparsons.com (R.M. Nagare), gerald.flerchinger@ars.usda.gov (G.N. Flerchinger).

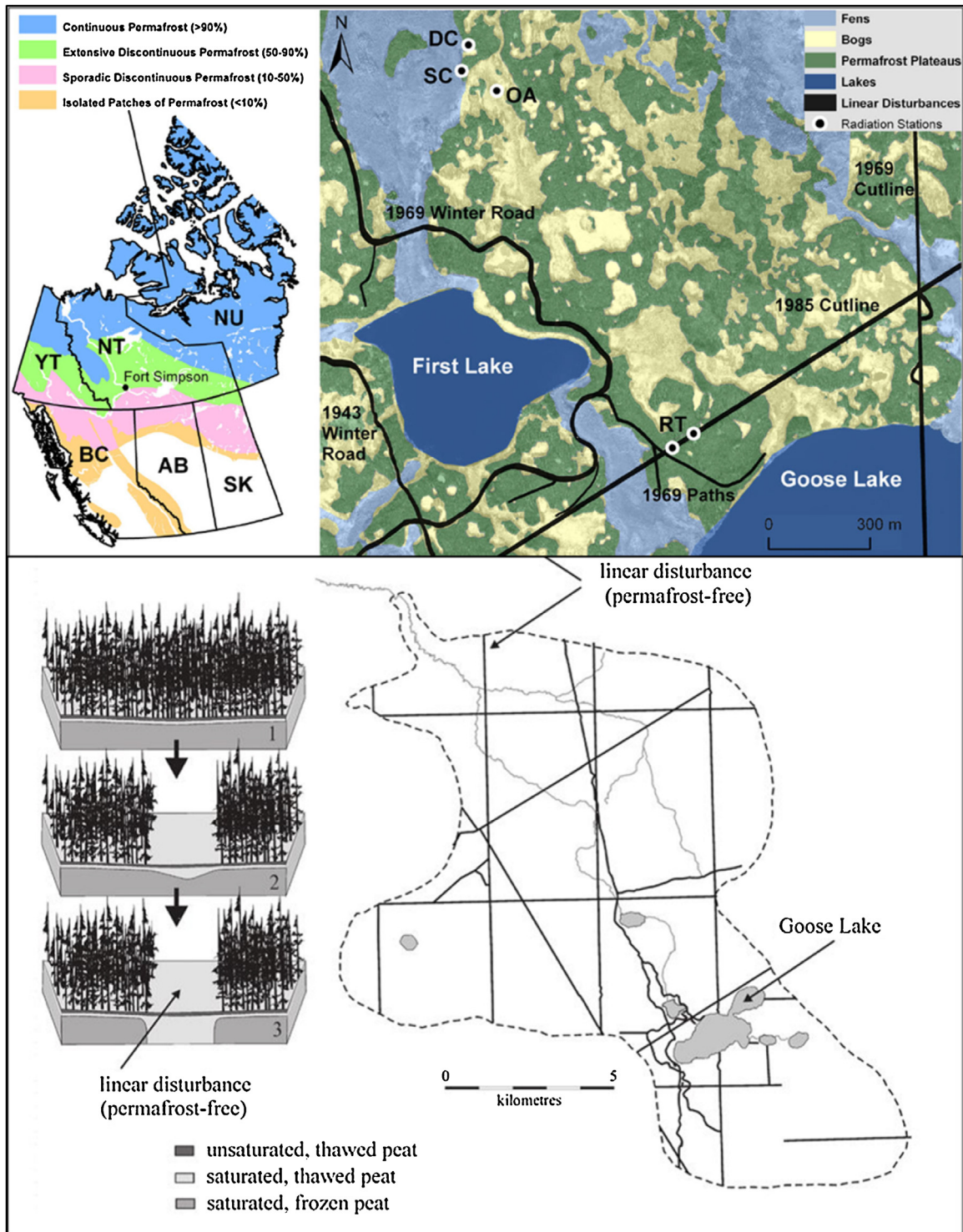


Fig. 1. Location of Scotty Creek near Fort Simpson, Northwest Territories within the zone of discontinuous permafrost and a plan view of the patterned peatland landscape (GSC, 2002). Lower images show plan schematic of linear disturbances at Scotty Creek along with a conceptual of permafrost thaw once the tree canopy has been removed (adapted from Quinton et al. (2009) and Williams and Quinton (2013)).

Robinson, 2003; Jorgenson et al., 2010; Williams et al., 2013). Seismic exploration involves the removal of the tree canopy and the compression of the ground surface, both of which decrease the thermal insulation of the active layer and permafrost (Wright et al., 2009). As a result, seismic lines typically represent lines of preferential permafrost thaw and ground surface subsidence.

In the wetland-dominated zone of discontinuous permafrost, permafrost occurs below tree-covered peat plateaus that rise 1–2 m

above surrounding treeless wetlands composed of flat bogs and channel fens (Wright et al., 2008). The presence and distribution of permafrost is correlated to mean annual air temperatures (MAAT) (Shur and Jorgenson, 2007), although peat plateaus and other organic soil-covered terrains in the southern margin of permafrost are highly effective at insulating permafrost so that permafrost can persist in areas of relatively high MAAT. Permafrost thickness ranges between 10 and 20 m and ground ice can constitute

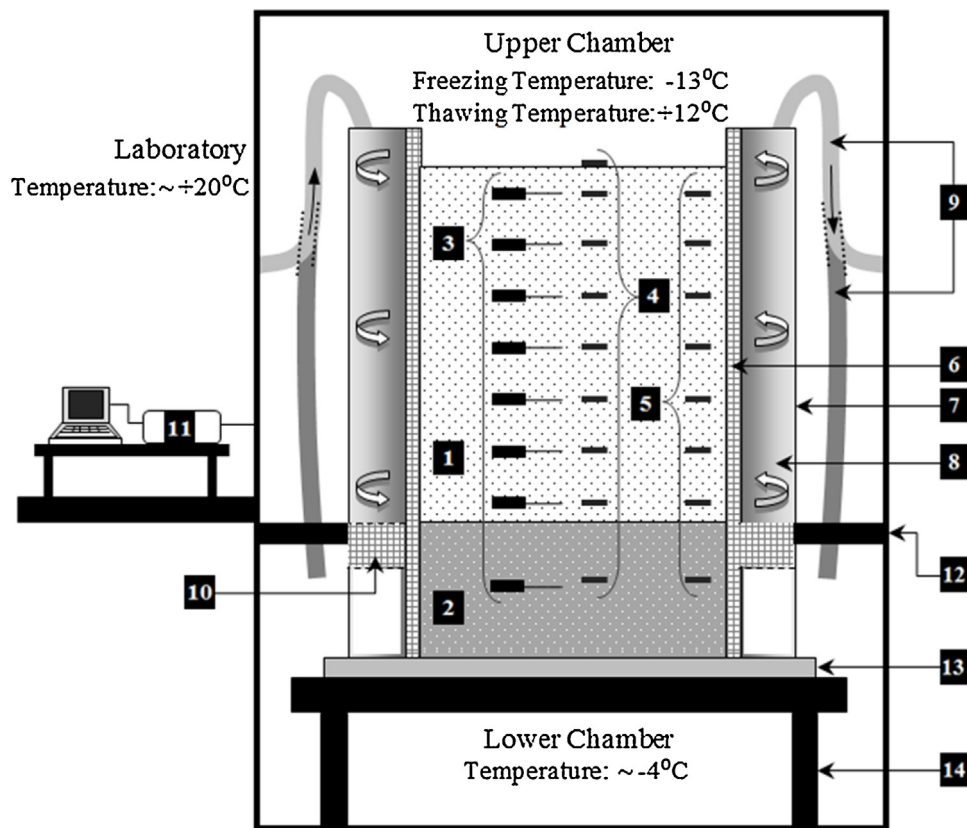


Fig. 2. Diagram showing experimental setup (not drawn to scale): (1) 65 cm deep active-layer, (2) 40 cm bottom frozen layer, (3) TDR probes, (4) Thermistor probes (centre), (5) Thermistor probes (edge), (6) Inner LDPE container lined with neoprene foam, (7) Outer LDPE container insulated with Reflectix® from outside, (8) Cavity in which air is circulated, (9) Ducting through which air is circulated into/out of the cavity, (10) 15 cm thick Neoprene band separating airspace from lower chamber, (11) Multiplexers and data-logger connected to a personal computer, (12) Adjustable insulated floor separating upper and lower chamber, (13) Weighing scale, (14) Frame to support monolith.

up to 80% of the plateau's volume, hence the raised elevation of the plateau surface. By the end of the thaw season, the water table is typically 0.3–0.5 m below the plateau ground surface, creating a shallow unsaturated zone (Wright et al., 2009). Subsurface flow through the active (i.e. seasonally thawed) layer is the main runoff pathway from plateaus (Wright et al., 2008). Bogs mainly store water as they are surrounded by raised, saturated permafrost. The water draining from plateaus is conveyed along channel fens towards the basin outlet (Hayashi et al., 2004).

The transition from fibric to well decomposed peat means hydraulic conductivity decreases exponentially with depth (Quinton et al., 2000). Therefore, the magnitude and timing of run-off is coupled with ground thaw depth (Quinton and Marsh, 1999; Hayashi et al., 2007). Active-layer thaw is driven by the ground heat flux, the fraction of the ground surface energy balance that is transferred into the subsurface (Woo and Xia, 1996). The main energy transfer process for the ground heat flux is thermal conduction (Hayashi et al., 2007), although advection may also contribute during snowmelt infiltration (Kane et al., 2001). Forcing is primarily top-down as heat is conducted along temperature gradients between the ground surface and underlying permafrost table. While air temperatures do affect ground thaw evolution, ground surface temperature (GST) controls the magnitude of the thermal gradient and its subsequent effect on subsurface temperatures. Air temperatures are only a proxy for radiation's effects on GST (Kurlylyk and Watanabe, 2013). Heat transport is tightly coupled with water movement, as the rate of ground thaw depends not only on the energy input at the surface but also on the thermal properties of the soil, which is strongly affected by soil moisture (Hayashi et al., 2007). Thus, the extent and distribution

of permafrost is also controlled by local meteorological and hydrological factors such as soil moisture, relief, incoming radiation and its effect on ground surface temperatures (Beilman and Robinson, 2003; Williams and Quinton, 2013). Conventional seismic surveys conducted during petroleum exploration effectively clears the tree canopy, creating linear tree-less corridors called seismic lines or cutlines (Quinton et al., 2009). Seismic exploration practices create 6–8 m wide cutlines, usually resulting in ground compaction and subsidence due to use of heavy machinery. Typically, when the canopy is removed the underlying permafrost begins to thaw. When the permafrost thaws, the ground ice disappears and the plateau collapses, resulting in considerable topographic changes (Wright et al., 2009). Thus, once permafrost is lost below these disturbances, they adopt new thermal, hydrological and ecological (vegetation) regimes (Williams et al., 2013).

Adopting best management practices is crucial to reducing impacts in areas of discontinuous permafrost where MAATs are closer to 0 °C and ground thermal regimes are more vulnerable to disturbance (Burgess and Smith, 2000; Williams and Quinton, 2013). One promising and relatively cost-effective mitigation measure is the application of mulch of the removed tree canopy, mainly black spruce (*Picea Mariana*), to cutlines once seismic surveys are complete. Mulching is appealing as a potential mitigation measure because mulch (in this case wood chips), lacks the capillarity to exhibit substantial matric potential and creates a drier ground surface with higher albedo (Oke, 2002). Reduced water retention capability results in lower bulk thermal conductivity which enables the mulch to act as a thermal buffer: a well aerated, low thermal conductivity layer insulating the permafrost below while also reflecting some solar radiation. Mulching has long been used to

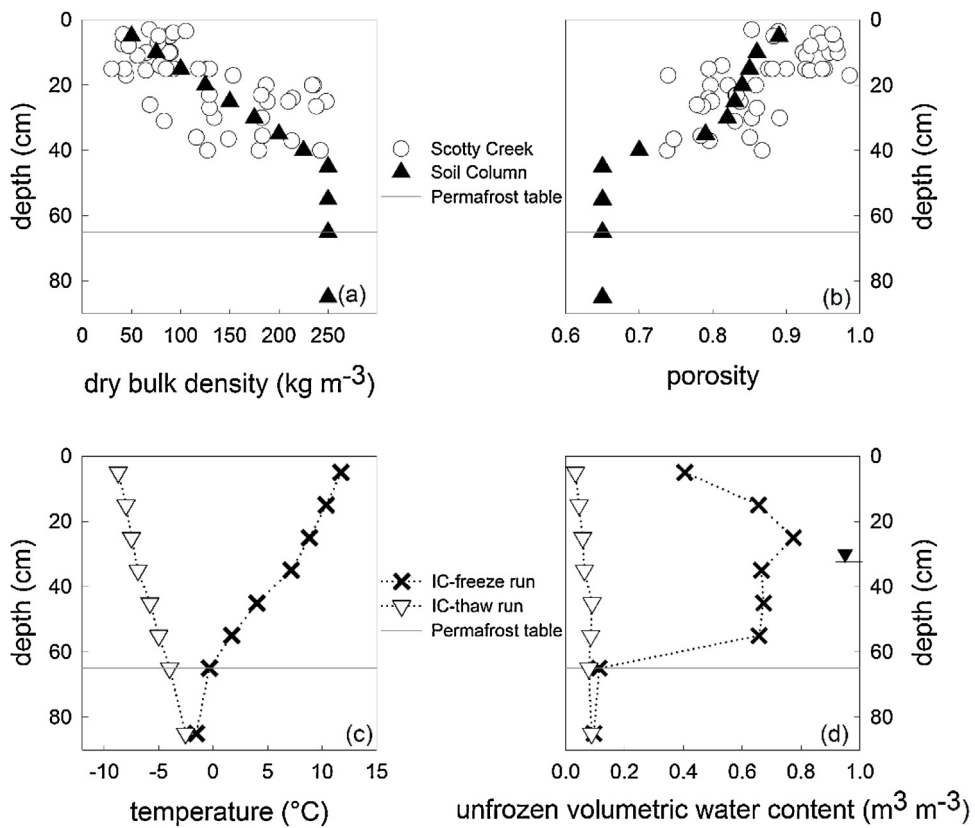


Fig. 3. (a) and (b) show the density and porosity profiles, Scotty Creek values obtained from Hayashi et al. (2007). (c) shows initial temperature profiles of soil column prior to the beginning of a freezing run and thawing run, denoted as IC (initial conditions)-freeze and IC-thaw. (d) shows initial water content profile of soil column for IC-freeze and IC-thaw runs; water table depth in the soil column experiment is indicated by the inverted triangle symbol at 35 cm, is only for the unfrozen condition (IC-freeze). Permafrost table depths on all plots are for the soil column experiment.

modulate soil temperatures, but influences on moisture and thermal regimes are complex as they are affected by mulch properties as well as local metrological and hydrological factors (Hillel, 1998).

Traditional agricultural mulches are usually applied in thin layers (≤ 10 cm) where their micro-topography, resistance to vapor transfer, and albedo play a dominant role in energy transfer (Oke, 2002; Sui et al., 1992; Fuchs and Hadas, 2011). Heat transfer through these mulches is a mixture of thermal conduction through the wood particles and convection by air in voids. However, the application of wood chips over permafrost, involves much thicker and denser layers that are better represented as a shallow variably-saturated porous media layer (Sui et al., 1992). Thus, air flow is minimized in these layers with thermal conduction being the prominent heat transport mechanism in pore-spaces in the absence of flowing water. When water is moving (e.g. infiltration), heat will also be transferred by advection. In peatlands, the mulch may also become saturated as the water table moves into and out of the layer. As such, for these circumstances, the mulch's moisture retention and thermal characteristics are best conceptualized as a porous media layer.

This study is aimed at investigating the effectiveness of mulching on thermally mitigating permafrost thaw below linear disturbances in organic-covered permafrost regions. This was achieved via a combination of laboratory and numerical model simulations of the seasonal freezing and thawing of a natural peatland based soil monolith. Laboratory experiments involved a large-scale soil column set-up, designed to investigate the key thermal and hydrological processes related to permafrost thaw in sub-arctic peatlands (Mohammed et al., 2014). This experiment was conducted in a two-level climate chamber specifically designed to realistically represent permafrost environments (Nagare et al.,

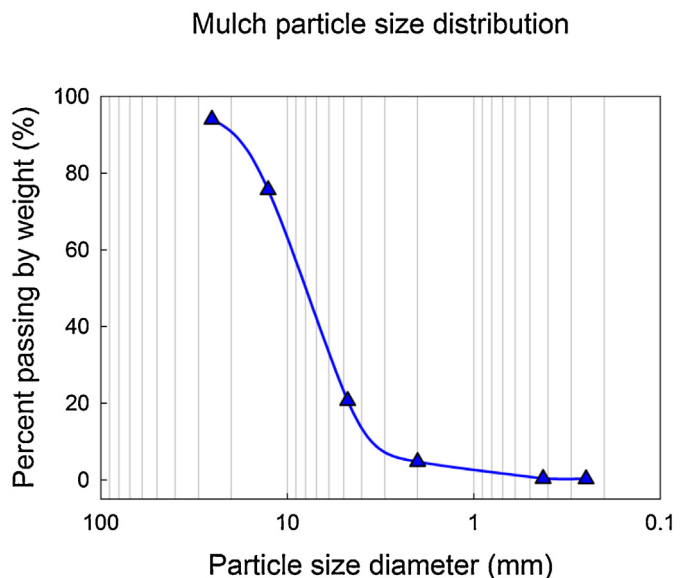


Fig. 4. Average particle distribution of black spruce mulch using in the soil column experiment.

2012a,b). The current study specifically tested the effect of mulch on reducing ground heat flux and slowing thaw progression. This was done by running freeze-thaw cycles with and without the mulch surface layer. The data were assimilated into the one-dimensional coupled soil water-energy transport model, SHAW (Simultaneous Heat and Water) (Flerchinger and Saxton, 1989).

Table 1

Definition and units for all variables used in Eqs. (1)–(6).

Symbol	Definition and respective units
b	Pore-size distribution parameter (unitless)
c_l	Specific heat capacity of water ($4200 \text{ J kg}^{-1} \text{ }^{\circ}\text{C}^{-1}$)
C_s	Volumetric heat capacity of soil ($\text{J m}^{-3} \text{ }^{\circ}\text{C}^{-1}$)
g	Acceleration due to gravity (9.81 m s^{-2})
k_s	Thermal conductivity of porous medium ($\text{W m}^{-1} \text{ }^{\circ}\text{C}^{-1}$)
K	Unsaturated hydraulic conductivity (m s^{-1})
K_s	Saturated hydraulic conductivity (m s^{-1})
L_f	Latent heat of fusion ($335,000 \text{ J kg}^{-1}$)
L_v	Latent heat of vaporization ($2,500,000 \text{ J kg}^{-1}$)
q_l	Liquid water flux (m s^{-1})
q_v	Water vapor flux ($\text{kg m}^{-2} \text{ s}^{-1}$)
t	Time (s)
T	Temperature ($^{\circ}\text{C}$)
T_K	Temperature (Kelvin)
U	Source/sink term for water flux equation ($\text{m m}^{-3} \text{ s}^{-1}$)
ϕ_i	Volumetric ice content of soil layer (m m^{-3})
ϕ_j	Volumetric fraction for j th soil constituent (m m^{-3})
ϕ_l	Volumetric liquid water content of soil layer (m m^{-3})
π	Osmotic potential of soil solution (m)
ρ_i	Density of ice (920 kg m^{-3})
ρ_l	Density of water (1000 kg m^{-3})
ρ_v	Vapor density of air space (kg m^{-3})
ρ_{vs}	Saturated vapor density (kg m^{-3})
ρ_{rs}	Vapor density at an exchange surface (kg m^{-3})
φ	Total water potential (m)
ψ	Soil water potential (m)
ψ_e	Soil air-entry potential (m)

Incorporating these data into the SHAW model allowed for key physical parameters important to simulating the process observed in the laboratory to be determined. The model, once calibrated and validated, was used to conduct an analysis on the combined effects of mulch thickness, moisture conditions and meteorological interactions (radiation, snowmelt and precipitation). This provided a basis to assess the effectiveness of the mitigation measure on its ability to slow permafrost thaw and for permafrost stabilization at disturbed areas.

2. Experimental description

2.1. Study region and problem description

Soil conditions simulated in this study aimed to replicate a peat plateau representative of the wetland-dominated zone of discontinuous permafrost. Climate information and soil characteristics, including soil temperature and moisture data measured at Scotty Creek, NWT (Fig. 1) were used as this reference. Scotty Creek drains an area of approximately 152 km^2 . The upper two-thirds of the drainage basin is dominated by peat plateaus, flat bogs and channel fens. The coverage of peat plateaus has decreased from about 70% in 1947 to approximately 40% in 2010, indicating a rapid rate of permafrost loss (Quinton et al., 2011). This rate of permafrost loss is typical of much of the southern fringe of permafrost, a region described in detail by Kwong and Gan (1994), and known to be highly vulnerable to climate and anthropogenic disturbances (Baltzer et al., 2014).

Linear disturbances range from 5 to 15 m in width, depending on the type of disturbance (CAPP, 2004; AECOM, 2009). The large network of seismic lines has a substantial footprint on the landscape (Fig. 1). Satellite image analysis by Quinton et al. (2011) of Scotty Creek revealed 133 km of linear disturbances (seismic lines and winter roads) within the 152 km^2 basin. This density of 0.875 km km^{-2} is about five times the natural drainage density of the channel fens and open channels within the basin, 0.161 km km^{-2} (Williams et al., 2013).

Williams and Quinton (2013) performed a study on the relative contributions of increasing incoming solar radiation and increases in soil moisture to permafrost thaw at linear disturbances at Scotty Creek. The authors concluded that the increase in incoming radiation at the ground surface is secondary compared to the increase in soil moisture and its effect on increasing ground heat flux to thaw underlying permafrost. Thus, the relatively low moisture content of the vadose zone enables it to insulate and maintain the underlying permafrost despite the warming atmosphere (Wright et al., 2009). Therefore, woody debris from the removed trees, when mulched and spread over the disturbed land should provide the slightly elevated relief and dryer ground conditions necessary to insulate and help preserve permafrost under the mulch (Williams, 2012). This hypothesis is supported by observations at Scotty Creek, and forms the basis of our study.

2.2. Climate chamber and soil mesocosm experiment

The climate chamber in which the soil column experiment was conducted is a two-level biome capable of simulating large-scale subsurface environments (Nagare et al., 2012a). The chamber consists of an upper and lower level allowing for soil columns to be placed between the two levels and separated by an adjustable insulated floor (Fig. 2). Situating part of the soil column in the lower chamber allows for the simulation of a saturated layer that remains frozen while the rest of the column in the upper chamber can be exposed to different climatic conditions. A full description of the climate chamber and its capabilities is described in Nagare et al. (2012a).

The soil column used in conjunction with the climate chamber utilized a column design that was able to simulate realistic vertical and lateral thermal boundary conditions on a variably-saturated peat monolith. The upper and lower chamber maintained permafrost and ground surface temperatures at the vertical ends of the soil column, while the active-layer portion of the soil column is insulated by an air-filled cavity. Temperature controlled air is circulated within the cavity matching the average temperature of the active layer as it underwent freezing and thawing. This design facilitated a controlled environment in which certain hydrological processes related to heat and water transfer in permafrost environments can be isolated and investigated without scaling requirements. A full description of the soil column design is presented in Mohammed et al. (2014).

The soil column was re-packed to match bulk density profiles from Scotty Creek in an effort to simulate a natural peatland profile characteristic of those in the region, while also allowing us to reproduce the additional effects of a linear disturbance, i.e. no tree canopy and ground compaction (Fig. 3). Ground compaction would result in the destruction of small-scale heterogeneities such as macropores and likely lower porosities. Time-domain reflectometry (TDR) probes (CS10 with SDMX multiplexers connected to a TDR100, Campbell Scientific Inc., Logan, UT) were used to measure unfrozen water content. Temperature sensors (107BAM with an absolute accuracy of $0.2\text{--}0.5 \text{ }^{\circ}\text{C}$, multiplexed using an AM16/32B, Campbell Scientific Inc.) were placed in the centre and edge of all instrumented depths (Figs. 2 and 3(c)). Calibration of the TDR probes utilized Maxwell-De Loor's four phase mixing model, details of which can be found in Nagare et al. (2011). All instrumentation was connected to a data logger (CR1000, Campbell Scientific Inc.) and values were measured and recorded every 15 min.

Temperatures were initially maintained at $20 \text{ }^{\circ}\text{C}$ and $-4 \text{ }^{\circ}\text{C}$ in the upper and lower chambers respectively, to establish stable temperature and water content profiles. A single freezing cycle was then initiated, lowering the upper chamber temperature to $-13 \text{ }^{\circ}\text{C}$ to simulate winter conditions. Once the column was completely frozen and the temperature profile relatively stable, the upper

Table 2

Soil texture and hydraulic parameters used in the SHAW model developed for this study. Note, depth intervals represent parametrization of the model, numerical discretization of the profile ranged from 2.5 to 10 cm to ensure numerical stability.

Parameter	Values used for different soil depths								
Depth (m)	+0.10 to +0.30	0.00–0.05	0.05–0.15	0.15–0.25	0.25–0.35	0.35–0.45	0.45–0.55	0.55–0.65	0.65–0.85
Texture	Mulch	Peat							
Sand (%)	0	0	0	0	0	0	0	0	0
Silt (%)	0	1	1	1	1	1	1	1	1
Clay (%)	0	1	1	1	1	1	1	1	1
Organic (%)	100	98	98	98	98	98	98	98	98
ρ_b (kg m ⁻³)	140	50	100	150	200	250	250	250	250
θ_s (m m ⁻³)	0.8	0.9	0.89	0.85	0.76	0.70	0.65	0.65	0.60
ψ_0 (m)	0.02	0.01	0.03	0.05	0.05	0.05	0.05	0.05	0.05
b	20.8	3.5	3.6	3.9	4.2	4.5	4.5	4.5	4.5
K_s (m s ⁻¹)	2.2×10^{-5}	3.0×10^{-5}	3.5×10^{-6}	3.0×10^{-7}	2.3×10^{-7}				
Albedo	0.35	0.25	–	–	–	–	–	–	–

Table 3

Summary of soil moisture and mulch combinations used in model analysis under the meteorological forcing data from Scotty Creek. All water table depths are measured below the ground surface.

Scenario	No Mulch		Mulch	
	Dry	Wet	Dry	Wet
Soil moisture	Dry	Wet	Dry	Wet
Water table depth (m)	−0.55	−0.05	−0.55	−0.05
Mulch thickness (m)	0	0	0.10–0.30	0.10–0.30

level temperature was sequentially increased from -13°C to 12°C , allowing 45 cm of the active-layer to undergo thawing. Freezing and thawing temperatures in this study represent approximately the average seasonal ground surface temperatures for the freezing and thawing periods at Scotty Creek (Wright et al., 2009). Initial water content and temperature distributions are shown in Fig. 3.

On completion of the first freeze-thaw cycle, the soil column was adjusted such that it matched the initial cycle's moisture and temperature conditions, and a second freeze-thaw run was then initiated. The only difference being the addition of a 20 cm layer of black spruce wood chip mulch to the thaw cycle. Rationalization for realistic mulch thicknesses were based on the volume of mulch available from chipping operations and its associated particle size distribution (Fig. 4). Scotty Creek supports an open mainly black spruce canopy of about 1 stem m⁻², with average heights and diameters being 3–5 m and 0.15 m, respectively (Wright et al., 2008; Williams et al., 2013). Using these numbers, and taking into account the porosity of the mulch (80%) when applied in the climate chamber, a maximum thickness of approximately 30 cm was calculated: thus 20 cm was deemed a conservative estimate. Comparison of the two thaw cycles allows a direct evaluation of the effect of the mulch on reducing ground thaw depth.

2.3. Numerical model

Computer modeling is widely used to investigate the response of hydrological systems to stresses due to climate and anthropogenic disturbances (Painter et al., 2013). However, natural hydrologic systems are complex and the isolation of key driving parameters can be difficult from field studies and the numerical models that are designed to represent them. The laboratory experiment discussed here was specifically designed to simulate the primary physical mechanism governing frost table progression – thermal conduction. It also represents the water and energy dynamics of a typical field system: variably saturated with water-ice phase change. In the field, isolating the influence of parameters on observations is difficult due to the simultaneous forcing from different hydrological and meteorological variables. Thus, data collected in the controlled laboratory experiment contain much less noise than present in field studies. This enables the quantification of the singular effect of

the mulch on impeding heat flux, and allows the simulation of a system that represents the key physical process governing ground thaw depths in these environments. Modeling can then play a vital role in understanding processes that may possibly include complex feedback mechanisms (Painter et al., 2013). The SHAW model was chosen for this study because of its strong physical basis for simulating surface water and energy fluxes, and coupled heat and water transfer through a 1-dimensional soil profile (Flerchinger and Saxton, 1989). It integrates the detailed physics of energy and water transfer within a plant canopy, snowpack, and soil profile including soil freezing and thawing. We present the fundamental equations and descriptions relevant to the modeling in this study below. All variables used in the equations are defined in Table 1. A detailed description of all physical processes represented in the model can be found in the technical documentation (Flerchinger, 2000). The energy balance at the ground surface is expressed as:

$$R_n + H + L_v E + G = 0 \quad (1)$$

where R_n is net all-wave radiation, H is sensible heat flux, $L_v E$ is latent heat flux, and G is soil or ground heat flux. The site's energy balance dictates how the Sun's radiant energy is partitioned for different surface and subsurface processes. Ground heat flux is the main source of energy for subsurface processes and is calculated as the residual of energy balance equation and must satisfy the heat flux equation for all nodes within the entire soil profile, which is listed below. Heat flux within the soil matrix is defined by:

$$C_s \frac{\partial T}{\partial t} - \rho_i L_f \frac{\partial \theta_i}{\partial t} = \frac{\partial}{\partial t} \left[k_s \frac{\partial T}{\partial z} \right] - \rho_i c_i \frac{\partial q_i T}{\partial z} - L_v \left(\frac{\partial q_v}{\partial z} + \frac{\partial q_l}{\partial t} \right) \quad (2)$$

where the terms on the left side represent the change in temperature and latent energy required to freeze water, and variables are as defined in Table 1. The terms on the right describe Fourier's law of heat conduction with the addition of advective heat transfer by infiltrating water and latent heat transfer by evaporation, respectively.

The thermodynamic equilibrium relationship between temperature and total water potential (matric plus osmotic) in soils during pore water phase change is represented by a form of the Clausius–Clapeyron equation that considers the latent heat of fusion (Fuchs et al., 1978):

$$\varphi = \pi + \psi = \frac{L_f}{g} \left(\frac{T}{T_K} \right) \quad (3)$$

Water flux within the soil is governed by a version of the Richards (1931) equation, modified for freezing and thawing soils:

$$\frac{\partial \theta_l}{\partial t} + \frac{\rho_i}{\rho_l} \frac{\partial \theta_i}{\partial t} = \frac{\partial}{\partial z} \left[K \left(\frac{\partial \psi}{\partial z} + 1 \right) \right] + \frac{1}{\rho_l} \frac{\partial q_v}{\partial z} + U \quad (4)$$

where the terms on the left side of the equation represent the change in volumetric liquid water and ice content, respectively. The

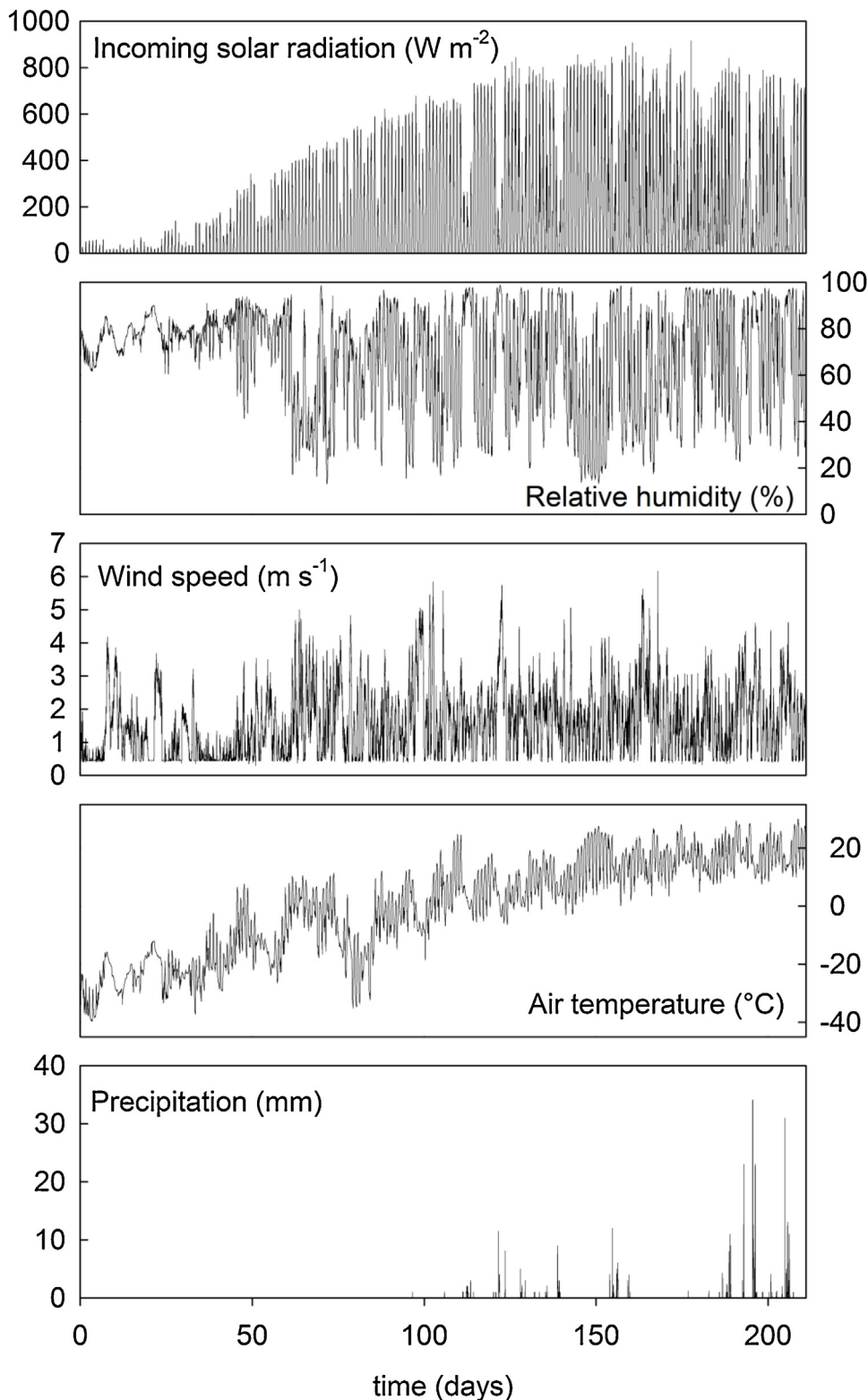


Fig. 5. Meteorological variables measured at Scotty Creek from January 1st, 2010 to August 1st, 2010, used to drive the SHAW model.

terms on the right side represent the net liquid influx in a layer, net vapor influx, and a source/sink term accounting for the water extraction by plants, respectively. Water flux is calculated as the product of the hydraulic conductivity times the soil matric potential

gradient. The unsaturated hydraulic conductivity is calculated in the SHAW model using the equation of [Campbell \(1974\)](#):

$$K = K_s \left(\frac{\theta_l}{\theta_s} \right)^{(2b+3)} \quad (5)$$

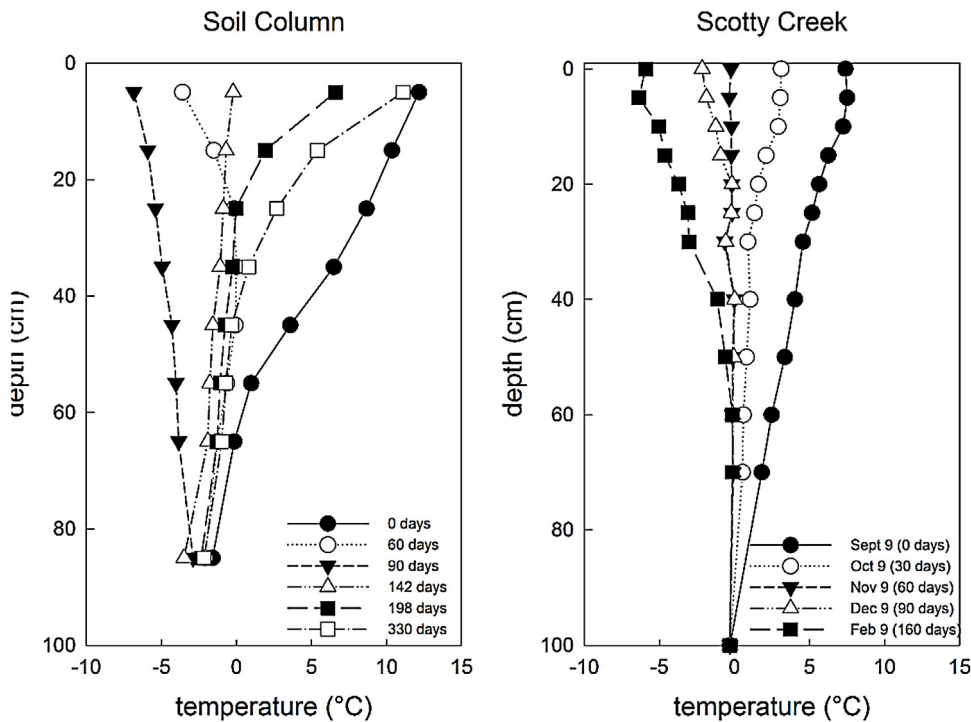


Fig. 6. Thermal regime over entire first freeze-thaw cycle for soil column experiment and Scotty Creek field site (November 2001–February 2002). The temperature at 100 cm depth for Scotty Creek is approximated from the Norman Wells pipeline (Smith et al., 2004).

and the Campbell (1974) equation is used to relate the soil moisture content to matric potential as:

$$\psi = \psi_e \left(\frac{\theta_l}{\theta_s} \right)^{(-b)} \quad (6)$$

2.4. Modeling procedure

Inputs used in the model included: initial conditions for soil temperature and water content profiles (Fig. 3-IC_thaw), hourly ground surface temperatures (GST), permafrost boundary temperatures (PBT), and physical characteristics of the soil and mulch. For the soil column experiment, version 2.7 of the SHAW model was modified to accept GST as the upper boundary rather than computing the full surface energy balance using meteorological inputs. The SHAW model was first applied to simulate the first freeze-thaw cycle without the mulch, and the associated heat and water transfer within the soil column experiment presented in Mohammed et al. (2014). This served as the calibration/validation dataset for the soil column parameters. The model was parameterized with measured values for most driving variables. Parameters that had to be estimated were used to calibrate the model, specifically the hydraulic retention parameters: air entry pressure (ψ_e) and Campbell pore-size distribution index (b). Simulations were forced with GST and permafrost temperatures measured at the ends of the soil column. The freezing period data was used to calibrate the model. The estimated parameters at the end of the calibration period were then used to validate the model against the thawing data.

Once the model was validated such that it represented reasonably well the rate of ground thaw observed in the first freeze-thaw cycle, it was then utilized to simulate the thawing portion of the second freeze-thaw cycle with the addition of the black spruce mulch (measured properties in Table 2 and Fig. 4). The mulch parameters were calibrated differently as there was no freezing cycle with added mulch. The mulch's measured water retention parameters obtained from tension infiltrometer experiments (described

below) were varied within the range of measured values to best fit the observed thaw cycle. Ensuring the model accurately captures the thermal effect of the mulch, observed in this controlled experiment, allows the effect of the mulch under differing meteorological conditions to be assessed.

Wood is hygroscopic, meaning it attracts and retains moisture (Tsoumis, 1991). Thus, the mulch's water transmission ability will vary with moisture content within matrix pores and also with the amount of moisture in the wood chips. Consequently, laboratory analyses were conducted to obtain moisture characteristics of the mulch at both saturated and unsaturated conditions, through tension infiltrometer experiments on samples packed to the same density used in the climate chamber. The infiltrometer results were assimilated into a MATLAB programme developed by Mollerup et al. (2008) which combines the Philip (1957, 1958) solution for 1D infiltration with a numerical inversion scheme to obtain the Campbell (1974) hydraulic retention parameters for the mulch (Table 2). As the study site is a wetland-dominated environment, it is reasonable to assume that the 'wet' mulch is more realistic of the hygroscopic extremes, and these were the parameters used.

The model was used to assess the effect of the mulch on impeding thaw progression, while being exposed to additional variables not simulated in the climate chamber. This was achieved by using available meteorological data measured at Scotty Creek to drive the calibrated model. Seismic best practice guidelines recommend that seismic surveys be conducted when the ground is still frozen. Thus, the modeling efforts were directed at replicating the effect of the mulch on a soil profile that captures initial conditions upon completion of a survey. The simulations replicate initial conditions prior to snow melt and were run from January 1st to August 1st (until time just after peak average air temperatures are reached) for a period of 210 days, with the initial temperature profile based on those in Fig. 6b. The driving variables included hourly values of air temperature (used as GST was unavailable), precipitation, relative humidity, wind speed and solar radiation measured at Scotty Creek (Fig. 5). In addition to investigating the response of the mulch to typical

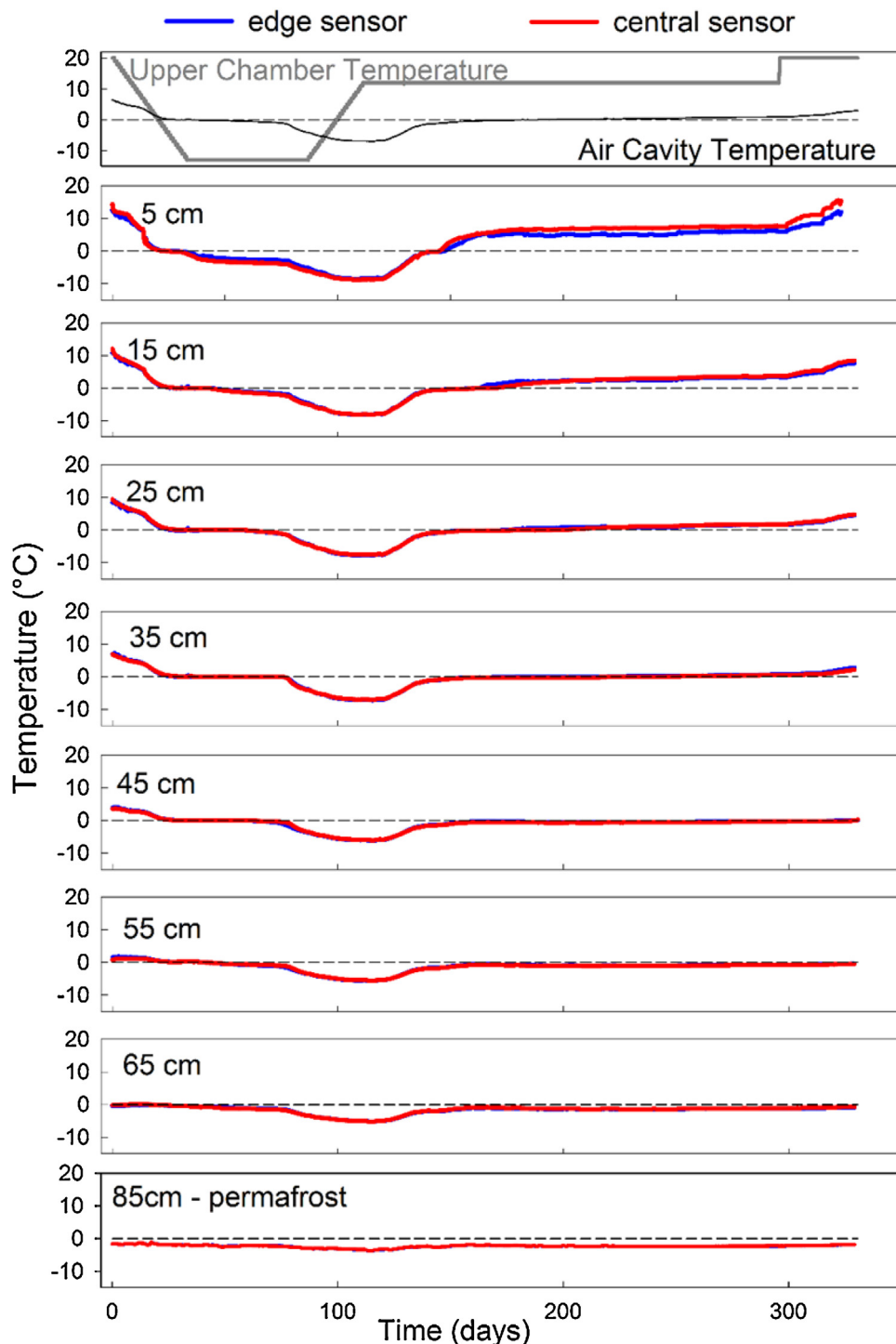


Fig. 7. Temperature time series for all instrumented depths (5–85 cm) in the soil column, as well as the upper chamber temperature and air cavity temperature at the top of the figure. Depths of each time series are listed in each graph. Central and edge sensors nearly completely overlap each other and thus edge sensor cannot be seen for 45 cm and deeper. Dashed line on all plots represent the 0 °C isotherm.

meteorological conditions, initial soil moisture distributions were varied as well in the simulations. Realistic wet and dry ground conditions were simulated, by initializing soil moisture profiles with values representative of a disturbed and undisturbed peat plateau, that is, relatively wet and dry conditions. This was done because soil moisture has a significant effect on the hydraulic and thermal properties of peat, and may consequently affect the evolution of the active-layer (Nagare et al., 2012b). Finally, the effects of differing mulch thicknesses were explored under the meteorological and

soil moisture scenarios. Table 3 summarizes the different scenarios simulated.

3. Results and discussion

3.1. Experimental results

The thermal regime of the monolith over the first freeze/thaw cycle without the mulch is shown in Fig. 6. Temperature time

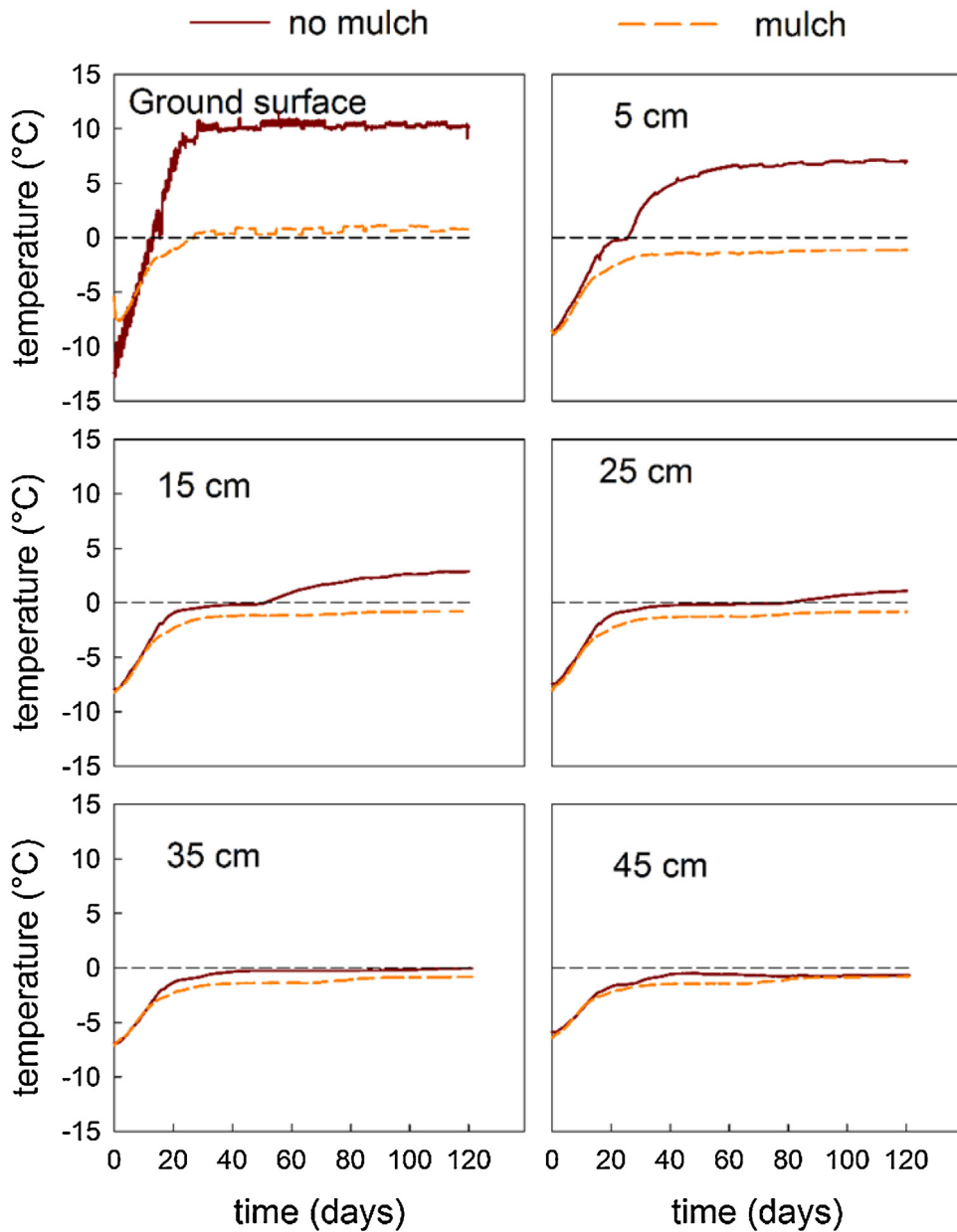


Fig. 8. Time series comparison of ground temperatures for all instrumented depths within the active-layer of the soil column during 125 days of the thaw period of the second experimental cycle with the added 20 cm mulch layer. Dashed line on all plots represent the 0 °C isotherm.

series (Fig. 7) highlight the experiment's capability to simulate one-dimensional heat transfer, which is discussed in Mohammed et al. (2014). A comparison of the temperature distributions produced in the laboratory soil column and at Scotty Creek illustrates the experiment's capability to reproduce the ground temperature conditions observed in the field (Fig. 6).

The thaw time in this study was approximately 200 days, comparing relatively well with the 156 days thawing period observed at the field site by Wright et al. (2009). Reasons for a longer thaw time are discussed in Mohammed et al. (2014) but in summary, are likely due to: (1) the absence of external sources of water (and thus energy) as the experiment did not simulate precipitation and snowpack, (2) the thawing temperature was held at 12 °C which represents the average thawing period temperature at Scotty Creek, and not the higher temperatures experienced in late summer which is when maximum thaw depths are reached (Wright et al., 2009), and, (3) the absence of a snowpack in this study resulted in evap-

oration beginning earlier in the thawing period than it would in the field. Decreases in moisture content and energy from the active layer due to evaporation, decreases the rate of heat conduction and slows thaw front progression. Another discrepancy may be due to the overestimation of frost depths measured by Wright et al. (2009) as measurements were taken with a frost probe. In the field, the active layer is often not saturated, and thus the frost probe may punch through parts of an unsaturated frozen profile and overestimate frost depths.

Thawing conditions in freeze-thaw cycle 2 (mulch layer) were identical to freeze-thaw cycle 1 (no mulch). Time-series data comparing the thermal evolution of the active layer for both thaw cycles for 125 days are shown in Fig. 8. Ground thaw for the no-mulch run began 13 days after the upper-level air temperatures increased and stabilized at 12 °C. In comparison, the mulched-surface run shows that thaw began after 27 days – a 14 day extension of the frozen

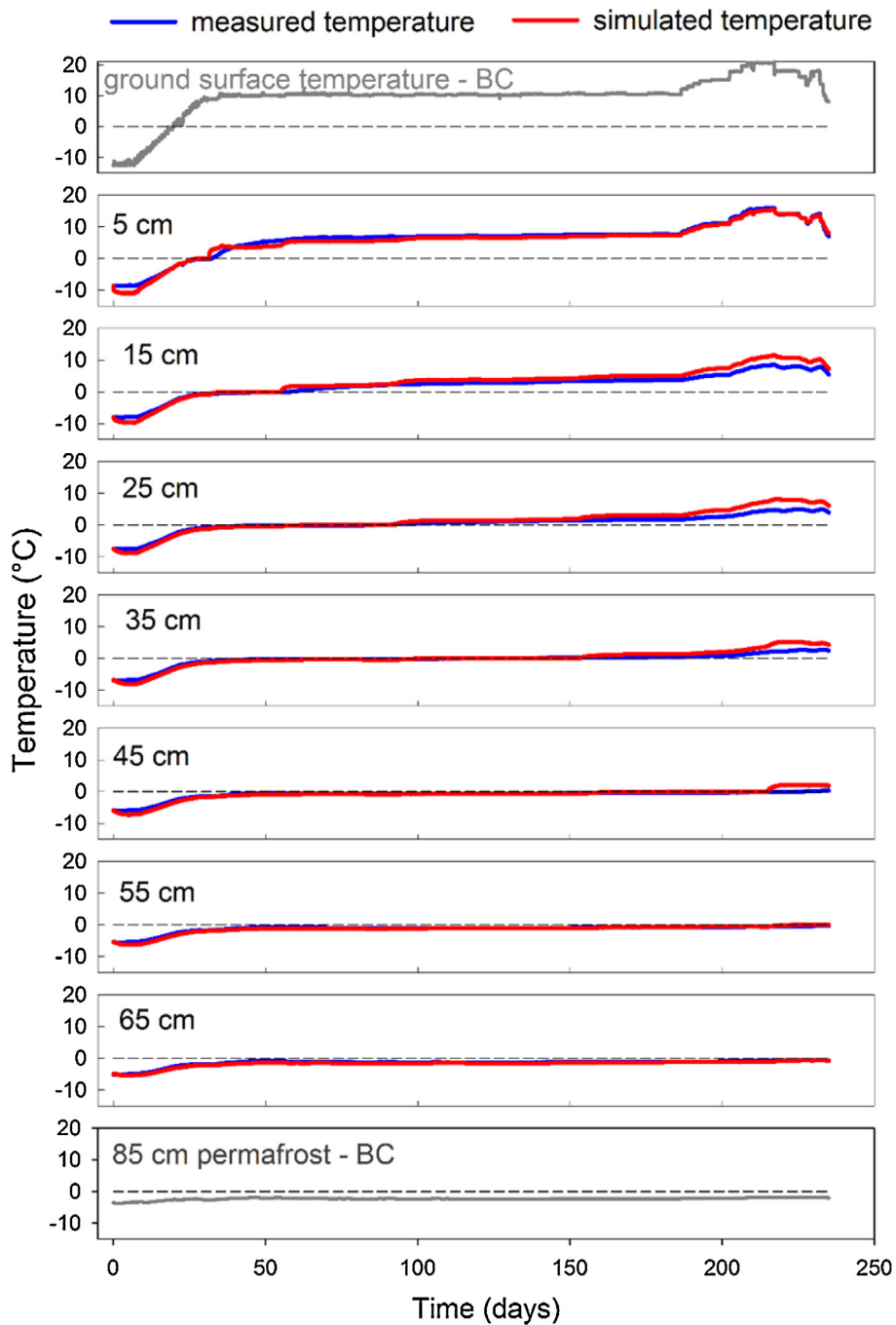


Fig. 9. Time series comparison of simulated vs. measured temperatures for all instrumented depths within the active-layer of the soil column during the thaw period of the first experimental cycle without added mulch. Temperature boundary conditions used in the model: ground surface temperatures and permafrost temperatures are shown in grey. Dashed line on all plots represent the 0 °C isotherm.

ground period. Thaw times for the no-mulch 5, 15 and 25 cm depths occurred 22, 52 and 81 days, respectively, while the corresponding depths for the mulch cycle never thawed. These depths did not thaw because of the temperature boundary conditions applied to the soil column. The boundary conditions replicated that of the no-mulch scenario, but the insulation ability of the mulch under the applied boundary conditions caused the system to reach a thermal steady state condition. Fig. 8 also shows that the temperature time series comparisons at all depths of the mulch cycle show slower warming rates compared to the no-mulch cycle (Fig. 8). The mulch clearly has an insulating effect on the soil's temperatures and slows thaw progression.

By removing the variability and inherent uncertainty of field data, the controlled mesocosm environment ensures that the only difference was the addition of the mulch. However, consequences of mulching based solely on these experiments are limited due to the absence of important meteorological processes not simulated, e.g. solar radiation, precipitation and snowpack. External sources of water (and thus energy), snowpack dynamics, and mid-winter thaw events can be very important mechanisms for active layer warming. Parameterized and validated with experimental data, incorporating these meteorological processes via numerical modeling enables effect of variables not simulated in the lab to be considered.

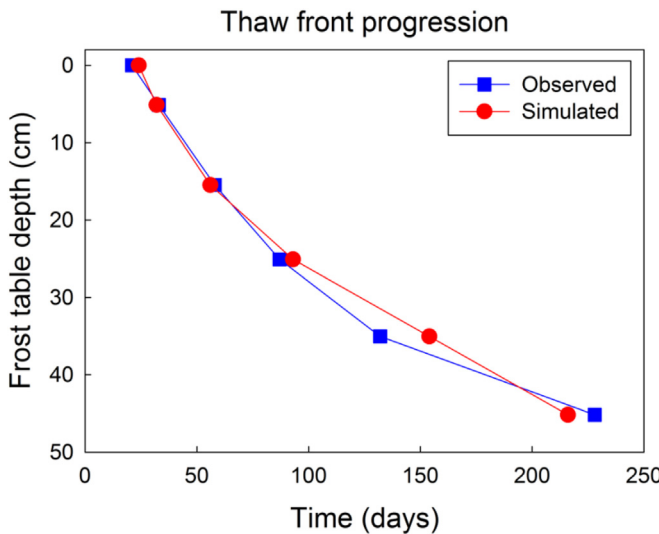


Fig. 10. Comparison of simulated vs. measured thaw progression in soil column.

3.2. Model evaluation

The experimental cycles with and without the mulch were used as part of the model evaluation process. The soil column portion of the model was calibrated using the freezing period data of the first cycle, and then evaluated against the subsequent thaw observations to validate it. It was only necessary to optimize hydraulic parameters in the simulations since the other main factors affecting heat transport (GST, PBT, soil texture and density) were directly measured. The accurate representation of water retention was critical to representing the ground heat flux due to the change in thermal conductivity with water content. The model was then used to simulate the thawing period without the mulch; Fig. 9 shows the comparison between modelled and measured temperatures. The largest discrepancies occur at the 15 cm and 25 cm depths and during the latter stages of the thawing period. The overestimation of temperatures towards the latter end of the thawing period could be due to the imposed temperature range in the climate chamber approaching the upper limits of the current experimental set-up's ability to maintain 1D thermal forcing. The greatest vertical range of temperatures within the active layer of the soil column occurred during the thaw cycle at the warmest temperatures. Portions of the soil column nearest the surface were then slightly cooler near the column edges because the air cavity temperature has to be less than higher soil temperatures to match the average temperature of the entire 65 cm column profile. Thus, it is reasonable to assume that those small lateral thermal gradients had a modulating influence on the vertical thermal gradient in the soil column (decreased slightly), which was not detected by the ground surface thermistor that provided the upper boundary for the model simulations. These deviations, from otherwise little or no difference in measured and modelled ground temperatures (Fig. 9), occurred when the upper chamber temperature was increased to 20 °C to perturb the approaching steady state thermal condition before ground thaw reached the desired 45 cm depth. The opposite is true, although to a much lesser degree for the freezing temperatures in the simulation, where there was a slight warming influence in the opposite direction. Despite these differences the model was still able to represent reasonably well the thaw progression in the active-layer (Fig. 10).

The mulch portion of the model was calibrated differently as there was no freezing cycle with added mulch. Water retention parameters obtained from the tension infiltrometer experiments were varied within the ranges of values measured to best fit the observed data. The Campbell pore-size distribution index (b),

the only parameter adjusted during this procedure, was varied between 20.0 and 22.8 until the best fit with observed data was achieved. Fig. 11 shows the comparison between modelled and measured temperatures for the second thaw cycle with added mulch. It can be seen that there is very little difference between the calibrated model and measured temperatures. Fig. 12 illustrates results on 1:1 plots for both thaw simulations of measured vs. simulated temperatures for all depths over the entire simulation period. Also shown in both figures are values for average root-mean squared residuals, which lie within the ranges presented in other studies (Daanen et al., 2007; McKenzie et al., 2007). Given these results, we believe it is reasonable to assume that the calibrated model is able to serve as a realistic analogue for heat transport in the mulch and soil column. Table 2 summarizes the parameters used in the final calibrated model; values were typical of other SHAW modeling studies in organic covered permafrost soils, including Scotty Creek (Zhang et al., 2008, 2010).

3.3. Simulated effect of mulch on ground thermal regime

Table 3 summarizes the different scenarios simulated to quantify the effect of the mulch on ground heat flux, thaw depth and soil temperature. The no-mulch scenario represents a generic peatland plateau profile underlying a seismic line, i.e. permafrost present and no tree canopy (due to removal). Because the model's lower temperature boundary condition is kept as the PBT in the soil column experiment, complete permafrost loss is not possible as temperatures are always <0 °C. Thus, while the lower boundary condition in the field will be affected by thaw, this is a conservative measure as the PBT essentially constrains the amount of possible thaw. As such it should be emphasized that the simulations are not exact predictions of how much the ground thaw will be advanced under the cut lines; they are a tool to explore the relative contributions of different mulch thicknesses under typical field conditions on ground thaw reduction. Fig. 13 illustrates the impact of the different mulch thicknesses on cumulative net ground heat flux, frost table progression and soil temperature distributions, respectively, for both dry and wet ground scenarios. It should be noted that thaw depths in this study were measured from the ground surface in all simulations, which was the 0 cm node for the 'no mulch' scenarios and the 10, 20 and 30 cm nodes for the different mulch thicknesses scenarios, respectively.

Ground heat flux is calculated as the residual of the surface energy balance in the SHAW model. Under both dry and wet soil conditions, the mulch acts to slow cumulative net ground heat flux and reduces the amount of energy being partitioned to thaw and warm the underlying soil over the thawing period. Closer inspection reveals that under all mulch scenarios, the cumulative net flux is negative compared to the no-mulch scenarios until approximately Days 124, 139, and 150 for the 10, 20 and 30 cm mulch thicknesses respectively. A negative net heat flux is indicative of heat being lost to the atmosphere as opposed to heat being conducted through the ground; and while this is certainly true for short time periods during the simulation, it should be noted that net heat flux in Fig. 13 is cumulative. The primary conclusion from these results is that the mulch produces a period of time (compared with the no-mulch scenario) when there is no net energy being input into the ground surface until net cumulative heat flux is positive. For both wet and dry scenarios, 10 and 20 cm thicknesses show similar trends in regards to reducing heat flux: 10 cm mulch decreases heat flux by 25 and 26%, and doubling mulch thickness to 20 cm produced a 32 and 33% heat flux reduction, for respective conditions. While a slightly larger change is seen with the 30 cm mulch under the wet scenario (45%), there is a noticeable divergence later in time for the dry soil profile and a much larger reduction results (62%). Overall, this net reduction of energy

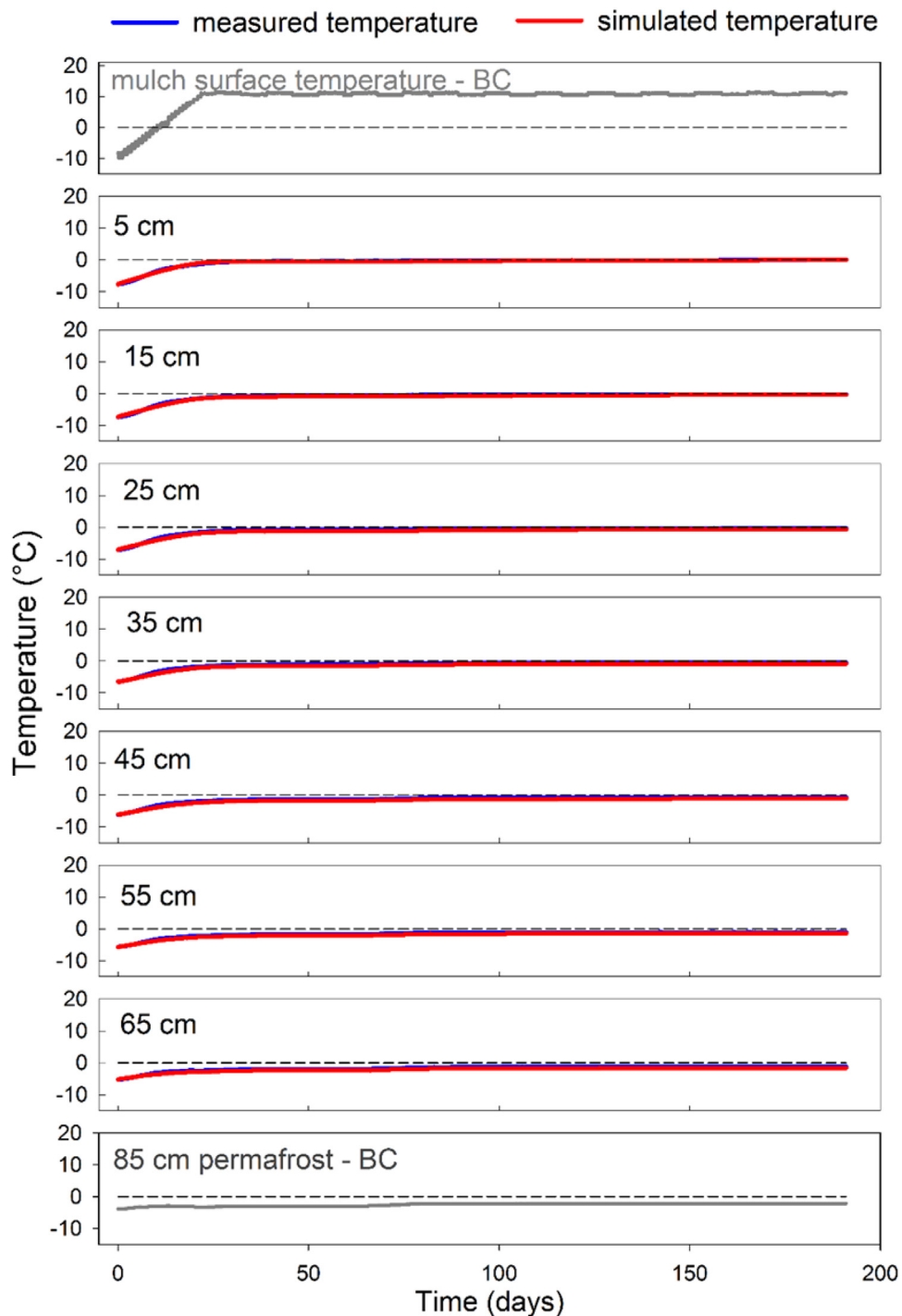


Fig. 11. Time series comparison of simulated vs. measured temperatures for all instrumented depths within the active-layer of the soil column during the thaw period of the second experimental cycle with the added mulch. Temperature boundary conditions used in the model: ground surface temperatures and permafrost temperatures are shown in grey. Dashed line on all plots represent the 0 °C isotherm.

input into the subsurface can be attributed to the low thermal conductivity of the mulch which slows the rate at which heat can be conducted from the atmosphere-ground surface interface to the underlying soil. Reducing the cumulative net heat flux is the first step towards offsetting permafrost thaw as it results in lower temperature regimes, provided other energy sources not simulated in this study (e.g. advection by laterally flowing water) remain the same.

The first major effect of mulching on ground thaw is the prolonged period of time the ground remains frozen during positive air

temperatures. Under the no-mulch scenarios, ground thaw began when the ground surface became snow free at approximately Day 47 and 53 for dry and wet ground conditions, respectively. However, the 10, 20 and 30 cm mulch thicknesses delayed ground thaw until approximately Days 110, 143 and 155 for both scenarios, respectively. This coincides closely to the periods when net heat flux becomes positive during the thaw period, and is expected as energy must be supplied for thaw to begin. Thaw depth fluctuations for short periods of time, most evident under the no-mulch scenarios, are a result of temperatures decreasing to below freez-

ing during approximately Days 111 and 140 (Fig. 13). This time is long enough for ground refreezing to occur before thaw is re-initiated. Under both scenarios, the mulch reduces the ability of surface temperature perturbations to penetrate the ground, which is evident as oscillations in thaw depth diminish with increasing mulch thicknesses. Under dry conditions, up until approximately Day 180, the 10, 20, and 30 cm depth thaw rate reductions are similar (i.e. slope and difference between the plot lines). The dry ground-10 cm mulch scenario shows reduced thaw only until Day 180. At this time under the no-mulch scenario, the thaw rate slows and begins to stabilize, reflecting the effect of solar radiation diminishing after the summer maximum and a brief period of cooler temperatures (Fig. 5). The thaw depth under the 10 cm-mulch goes deeper in after this time and performs worse as thaw continues its downward progression. The lack of thaw reduction under the 10 cm mulch compared to the no-mulch scenario is likely due to the no-mulch treatment being able to transmit the reduced energy input (cooler temperature and reduced solar radiation) around day 180 more rapidly into the soil profile than the mulch treatments. The mulch treatments cause a much greater time lag for temperature pulses being transmitted into the soil profile. Thaw continues to move deeper in the mulch scenarios due to heat stored within the profile. This effect is negated with the application of the thicker 20 and 30 cm mulch treatments as they show reduced thaw for the entire period. The 20 and 30 cm mulch treatments resulted in a 12 and 37% reduction in thaw depth, respectively. The overall reduced ground heat flux over the entire simulation period offsets the amount heat stored in the soil column as radiation and air temperatures begin to diminish from their maximum.

Under the wet soil scenario all simulated mulch thicknesses showed reduced thaw. Again, similar to the dry ground conditions, the application of the mulch insulates the underlying soil and delays thaw initiation. However, in the wet ground scenario, because of the larger amount of water present compared to the dry scenario, the soil column requires more latent heat to melt ground ice. The reduction of available heat flux and the thermal buffering capacity of the mulch, combined with the larger amount of ice, extends the zero-degree curtain period and increases the time to thaw soil layers. Because of this, thaw reduction is larger than dry ground scenarios, resulting in 42, 58 and 71% reduction for the 10, 20 and 30 cm mulch thicknesses, respectively.

In summary, for both scenarios, the prolonged soil thawing period also resulted in the mulch subsurface temperature remaining cooler compared to no-mulch scenarios (Fig. 13). This again is linked to the combined effects of lower cumulative heat flux and insulation, both attributed to the addition of the mulch. The diminished energy input to ground heat flux means that upon thaw, less sensible heat is available for warming and thus ground temperatures remain cooler with the mulch layer.

4. Conclusions

Mulching over seismic lines is an effective practice to reduce the impact of linear disturbances on permafrost degradation in peatlands of Northern Canada, located along the southern fringe of the Arctic permafrost region. A soil monolith-climate chamber experiment investigated the effects mulch on mitigating permafrost thaw. Running freeze-thaw simulations with and without the mulch enabled its effect on impeding ground heat flux to be tested. The data were assimilated into a coupled heat and water transport model, allowing the quantification of important parameters controlling the process observed in the lab study. Using field measured meteorological data to drive the model, simulations investigated the combined effects of mulch thickness, antecedent moisture conditions and meteorological interactions. This provided a basis to

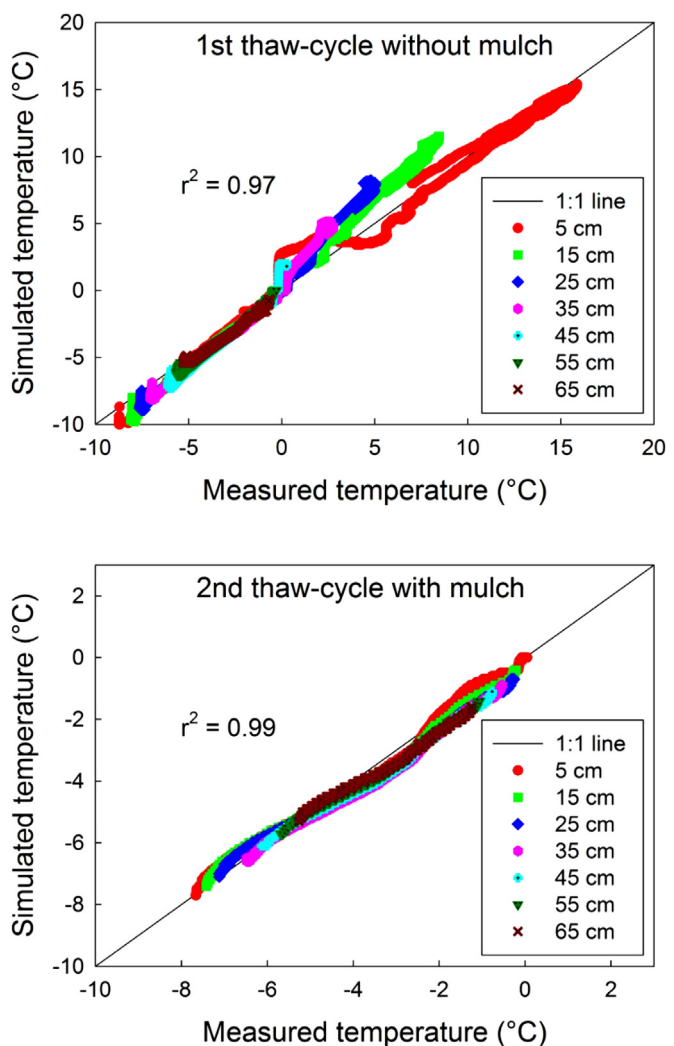


Fig. 12. (a) Scatter plot of simulated vs. measured temperature values for all depths within the active-layer of the soil column. (b) Scatter plot of simulated vs. measured thaw progression times for all depths within the active-layer of the soil column.

assess the mitigation measure on its ability to reduce the rate of permafrost thaw. Results demonstrate the ability of the mulch to decouple the subsurface thermal regime from meteorological forcing by impeding ground heat flux. This is due to the mulch acting as a low thermal conductivity layer. The mulch acts to insulate the ground surface, prolonging the period the ground remains frozen and delaying thaw initiation. The lab mesocosm study clearly illustrated the insulating effect a mulch layer has on slowing heat conduction. This was highlighted by cooler soil temperatures and slower thaw progression compared with the no-mulch scenario. A key objective of the experimental set-up was to replicate soil freeze-thaw processes at an appropriate representative elementary volume (REV) that would realistically capture coupled heat and water transport in these permafrost environments. Thus, the large REV of the monolith and the ability to impose field-scale boundary conditions (Mohammed et al., 2014), means that the validity of the experimental results should hold regardless of the width of the disturbance.

The numerical modeling efforts were aimed at reproducing the effect of the mulch on a soil profile that replicated field conditions. The end of the simulation period was chosen to be the time just after solar radiation and air temperatures are highest, and when active layer depths are deepest. The simulation thus captures the period when ultimate thaw depths are reached for the year and per-

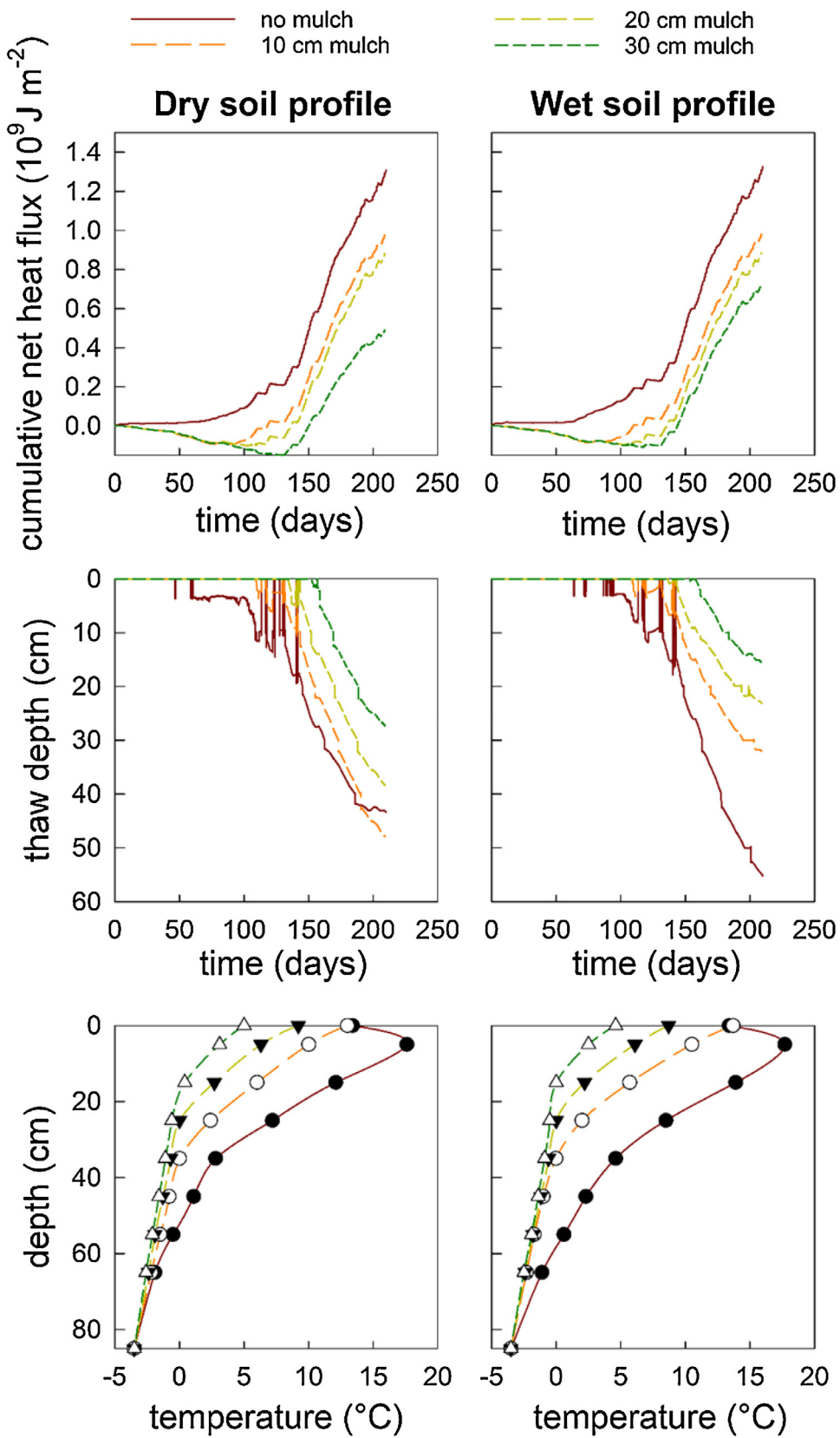


Fig. 13. Cumulative net ground heat flux, ground thaw progression and soil column temperature distributions during the simulated thawing period or dry (left column) and wet soil (right column) scenarios under 0–30 cm of mulch.

mafrost is most susceptible to increased thaw, and when the mulch layer makes a difference in thaw depth reduction. The simulations, initialized during the winter period, show that upon positive air temperatures, the mulch insulates the soil profile and prolongs the time before ground thaw begins. The extension of the frozen ground period is directly attributed to the mulch's ability to effectively reduce the amount of energy being partitioned into ground heat flux; the mulch increases the period of time before there is a net addition of energy to the subsurface. As there must be an input of energy to initiate thaw, this will almost always ensure reduction in thaw depths. Results indicate that different mulch thicknesses show similar thaw reducing ability except under specific conditions and during certain time periods. Under dry conditions, the 10 cm mulch did not have a positive effect on reducing ground thaw. This is likely due to the mulch's thermal inertia, resulting in a time lag before the soil began feeling the cooling effects of reduced radiation and temperature. Under wet conditions, however, all simulated mulch depths showed reduced thaw. Aside from the dry ground-10 cm mulch scenario, thaw reduction ranged from 12 to 71%, with the wet ground-30 cm mulch scenario achieving the maximum thaw depth reduction. Mulching also resulted in the subsurface temperature remaining cooler compared to no-mulch scenarios. The consequence of linear disturbances most detrimental to permafrost thaw is the increase in soil moisture (Williams and Quinton, 2013). Thus the wet scenario, where the soil profile 5 cm below the ground surface was saturated, represents a potentially 'worst case' situation where soil moisture and thermal conductivity are the highest. Under this scenario, all mulch thicknesses were still able to reduce ground thaw and maintain cooler thermal regimes. The overall result of its application is less energy being partitioned into ground heat flux by decreasing the rate of heat conduction to the frost table, reducing energy available for permafrost thaw and thus slowing thaw front progression. Based on these simulation results, mulching at higher application rates appears to have the potential to keep much of the peat below frozen throughout the summer season until air temperatures drop below freezing again. This suggests that mulching over aging disturbances, such as seismic lines where permafrost is very degraded, may have the potential to stabilize thaw or even regenerate permafrost. Similarly, mulching over disturbances while the ground is still frozen or prior to complete active-layer thaw, should result in minimized disturbance to the thermal state of the permafrost.

While results validate the insulative ability of the mulch, the above analyses do have limitations. There remain uncertainties regarding the persistence and evolution of the mulch properties over time. Degradation of the mulch will likely affect its physical characteristics, for example aging mulch may lower its albedo, and as such these changes will have effects on the mulch's capability. At some point the mulch will surely degrade to the point that it becomes a woody layer in the peat, much like any other spruce litter in these environments. Under these conditions, once drier ground conditions persist, the mulch should not have any detrimental effects on canopy regeneration. Subsurface run-off within the mulch was not simulated as SHAW is only a 1D model. As shallow subsurface flow is the main run-off mechanism on plateaus, and when frost table depths are shallow early in the thaw season, run-off will likely be within the mulch at some point. The effects of different topographic relief and laterally flowing pore-water through the mulch remain unknown and should be further studied.

The results are difficult to extend beyond the scenarios described, due to the limitations highlighted, and further field studies on mulching as a best management practice are warranted. Identifying these uncertainties will help to further characterize the effect of the mulching technique at the basin scale, and its persistence over time. However, the ability of the mulch to limit the

initial disturbance to the ground thermal regime and subsequently conserve permafrost is encouraging. It is the sustained additional energy being supplied over linear disturbances for ground heat flux over many years that contributes to complete permafrost loss and its associated hydrological and ecological impacts. Climate-chamber and numerical experiments investigating the mulch's effect on ground heat flux indicate reduced ground thaw and cooler subsurface temperatures, which should reduce the impact of the disturbances. As such, mulching should be an effective technique to reduce permafrost degradation in sub-arctic peatland regions. This is a major issue in cold region studies due to the tight coupling of heat and water movement, and non-linear feedbacks that control the hydrological and ecological cycles of these environments. This lab and modeling study, coupled with field data to constrain and validate parameters, provides a scientific basis to the resource management practice of mulching over seismic lines, and will aid in ensuring that the inevitability of increased northern exploration is performed in a more environmentally conscious and sustainable manner.

Acknowledgements

The authors wish to acknowledge the financial support of the Natural Science and Engineering Research Council of Canada (NSERC) and BioChambers Inc. (MB, Canada) through a NSERC-CRD award, NSERC Strategic Projects grant, and the Canadian Space Agency (CSA) through a Capacity Building in SS&T Cluster Pilot grant. We also thank Roger Peters, Steve Bartlett, Jon Jacobs and Marc Schincariol for their assistance in the laboratory.

References

- AECOM, 2009. *Considerations in Developing Oil and Gas Industry Best Practices in the North*, Environmental Studies Research Report No. 175. Government of Canada, Whitehorse, YT36.
- Aylsworth, J.M., Kettles, I.M., Todd, B.J., 1993. Peatland distribution in the Fort Simpson area, Northwest Territories with a geophysical study of peatland-permafrost relationships at Antoine Lake. *Curr. Res. Geol. Survey Can. Paper 93-1E*, 141–148.
- Baltzer, J.L., Veness, T., Chasmer, L.E., Sniderhan, A.E., Quinton, W.L., 2014. Forests on thawing permafrost: fragmentation, edge effects, and net forest loss. *Global Change Biol.* 20, 824–834, <http://dx.doi.org/10.1111/gcb.12349>.
- Beilman, D.W., Robinson, S.D., 2003. Peatland permafrost thaw and landform type along a climate gradient. In: Phillips, M., Springman, S.M., Arenson, L.U. (Eds.), *Proceedings of the Eighth International Conference on Permafrost*, vol. 1. A.A. Balkema, Zurich, Switzerland, pp. 61–65.
- Burgess, M.M., Smith, S.L., 2000. Shallow ground temperatures. In: Dyke, L.D., Brooks, G.R. (Eds.), *The Physical Environment of the Mackenzie Valley, Northwest Territories: A Base Line for the Assessment of Environmental Change*. Geological Survey of Canada, Ottawa, pp. 89–103.
- Campbell, G.S., 1974. A simple method for determining unsaturated conductivity from moisture retention data. *Soil Sci.* 17, 311–314.
- Canadian Association of Petroleum Producers (CAPP), 2004. *Geophysical Exploration Practices*, pp. 4.
- Daanen, R.P., Misra, D., Epstein, H., 2007. Active-layer hydrology in nonsorted circle ecosystems of the arctic tundra. *Vadose Zone J.* 6, 694–704.
- Flerchinger, G.N., 2000. The Simultaneous Heat and Water (SHAW) Model: Technical Documentation, Technical Report NWRC 2000-09.
- Flerchinger, G.N., Saxton, K.E., 1989. Simultaneous heat and water model of a freezing snow-residue-soil System. 1. Theory and Development. *Trans. ASAE* 32, 569–571.
- Fuchs, M., Campbell, G.S., Papendick, R.I., 1978. An analysis of sensible and latent heat flow in a partially frozen unsaturated soil. *Soil Sci. Soc. Am. J.* 42 (3), 379–385.
- Fuchs, M., Hadas, A., 2011. Mulch resistance to water vapor transport. *Agric. Water Manag.* 98, 990–998.
- Geological Survey of Canada (GSC), 2002. Permafrost Thickness in Canada, www.geografis.cgd.gc.ca.
- Hayashi, M., Quinton, W.L., Pietroniro, A., Gibson, J.J., 2004. Hydrologic functions of wetlands in a discontinuous permafrost basin indicated by isotopic and chemical signatures. *J. Hydrol.* 296, 81–97.
- Hayashi, M., Goeller, N., Quinton, W.L., Wright, N., 2007. A simple heat conduction method for simulating the frost table depth in hydrological models. *Hydrol. Process.* 21, 2610–2622.
- Hillel, D., 1998. *Environmental Soil Physics*. Academic Press, New York, 771pp.

- Jorgenson, J., Hoef, J., Jorgenson, M., 2010. Long-term recovery patterns of arctic tundra after winter seismic exploration. *Ecol. Appl.* 20, 205–221.
- Kane, D.L., Hinkel, K.M., Goering, D.J., Hinzman, L.D., Outcalt, S.I., 2001. Nonconductive heat transfer associated with frozen soils. *Global Planet. Change* 29, 275–292.
- Kurlylyk, B.L., Watanabe, K., 2013. The mathematical representation of freezing and thawing processes in variably-saturated, non-deformable soils. *Adv. Water Resour.* 16, 160–177.
- Kwong, Y.T.J., Gan, T.Y., 1994. Northward migration of permafrost along the Mackenzie highway and climate warming. *Clim. Change* 26 (4), 399–419.
- McKenzie, J.M., Voss, C.I., Siegel, D.I., 2007. Groundwater flow with energy transport and water–ice phase change: numerical simulations, benchmarks, and application to freezing in peat bogs. *Adv. Water Resour.* 30, 966–983.
- Mohammed, A.A., Schincariol, R.A., Nagare, R.M., Quinton, W.L., 2014. Reproducing field scale active layer thaw in the laboratory. *Vadose Zone J.* 13 (8), <http://dx.doi.org/10.2136/vzj2014.01.0008>.
- Mollerup, M., Hansen, S., Petersen, C., Kjaersgaard, J.H., 2008. A MATLAB program for estimation of unsaturated hydraulic soil parameters using an infiltrometer technique. *Comput. Geosci.* 34, 861–875.
- Nagare, R.M., Schincariol, R.A., Quinton, W.L., Hayashi, M., 2011. Laboratory calibration of time domain reflectometry to determine moisture content in undisturbed peat samples. *Eur. J. Soil Sci.* 62, 505–515.
- Nagare, R.M., Schincariol, R.A., Quinton, W.L., Hayashi, M., 2012a. Moving the field into the lab: simulation of water and heat transport in subarctic peat. *Periglac. Process.* 23, 237–243.
- Nagare, R.M., Schincariol, R.A., Quinton, W.L., Hayashi, M., 2012b. Effects of freezing on soil temperature, freezing front propagation and moisture redistribution in peat: laboratory investigations. *Hydrol. Earth Syst. Sci.* 16, 501–515.
- Oke, T.R., 2002. *Boundary Layer Climates*. Routledge.
- Painter, S.L., Moulton, J.D., Wilson, C.J., 2013. Modeling challenges for predicting hydrologic response to degrading permafrost. *Hydrogeol. J.* 21, 221–224.
- Philip, J.R., 1957. The theory of infiltration: 1. The infiltration equation and its solution. *Soil Sci.* 83, 345–357.
- Philip, J.R., 1958. The theory of infiltration: 6. Effect of water depth over soil. *Soil Sci.* 85, 278–286.
- Quinton, W.L., Gray, D.M., Marsh, P., 2000. Subsurface drainage from hummock-covered hillslope in the Arctic tundra. *J. Hydrol.* 237, 113–125, [http://dx.doi.org/10.1016/S0022-1694\(00\)00304-8](http://dx.doi.org/10.1016/S0022-1694(00)00304-8).
- Quinton, W.L., Marsh, P., 1999. A conceptual framework for runoff generation in a permafrost environment. *Hydrol. Process.* 13, 2563–2581.
- Quinton, W.L., Hayashi, M., Chasmer, L.E., 2009. Peatland hydrology of discontinuous permafrost in the Northwest Territories: overview and synthesis. *Can. Water Resour. J.* 34 (4), 311–328.
- Quinton, W.L., Hayashi, M., Chasmer, L.E., 2011. Permafrost-thaw-induced land-cover change in the Canadian subarctic: implications for water resources. *Hydrol. Process. Sci. Brief.* 25, 152–158, <http://dx.doi.org/10.1002/hyp.7894>.
- Richards, A.L., 1931. Capillary conduction of liquids through porous media. *Physics* 1, 316–333.
- Shur, Y.L., Jorgenson, M.T., 2007. Patterns of permafrost formation and degradation in relation to climate and ecosystem. *Permafro. Periglac. Process.* 18, 7–19.
- Smith, S.L., Burgess, M.M., Riseborough, D., Coultsch, T., Chartrand, J., 2004. Digital Summary Database of Permafrost and Thermal Conditions – Norman Wells Pipeline Study Sites. *Geol. Survey Can. (GSC) Open File*, 4635.
- Sui, H., Zeng, D., Chen, F., 1992. A numerical model for simulating the temperature and moisture regimes of soil under various mulches. *Agric. For. Meteorol.* 61, 281–299.
- Tarnocai, C., 2006. The effect of climate change on carbon on Canadian peatlands. *Global Planet. Change* 53, 222–232.
- Tsoumis, G., 1991. *Science and Technology of Wood*. Van Nostrand Reinhold, New York, 494pp.
- Williams, T.J., M.Sc. Thesis 2012. Recovery of Linear Disturbances in a Discontinuous Permafrost Peatland Environment. Wilfred Laurier University, Canada.
- Williams, T.J., Quinton, W.L., Baltzer, J.L., 2013. Linear disturbances on discontinuous permafrost: implications for thaw-induced changes to land cover and drainage patterns. *Environ. Res. Lett.* 8, <http://dx.doi.org/10.1088/1748-9326/8/2/025006>, 12pp.
- Williams, T.J., Quinton, W.L., 2013. Modelling incoming radiation on a linear disturbance and its impact on the ground thermal regime in discontinuous permafrost. *Hydro. Process.*, <http://dx.doi.org/10.1002/hyp.9792>.
- Woo, M.K., 1986. *Permafrost hydrology in North America*. *Atmosphere–Ocean* 24, 201–234.
- Woo, M.K., Winter, T.C., 1993. The role of permafrost and seasonal frost in the hydrology of wetlands in North America. *J. Hydrol.* 141, 5–31.
- Woo, M.-K., Xia, Z., 1996. Effects of hydrology on the thermal conditions of the active layer. *Nordic Hydrol.* 27, 429–448.
- Wright, N., Quinton, W.L., Hayashi, M., 2008. Hillslope runoff from an ice-cored peat plateau in a discontinuous permafrost basin, Northwest Territories, Canada. *Hydro. Process.* 22, 2816–2828.
- Wright, N., Hayashi, M., Quinton, W.L., 2009. Hillslope runoff from an ice-cored peat plateau in a discontinuous permafrost basin, Northwest Territories, Canada. *Water Resour. Res.* 45, W05414.
- Zhang, Y., Carey, S.K., Quinton, W.L., 2008. Evaluation of the algorithms and parameterizations for ground thawing and freezing simulation in permafrost regions. *J. Geophys. Res.–Atmos.* 113, D17116.
- Zhang, Y., Carey, S.K., Quinton, W.L., Janowicz, J.R., Pomeroy, J.W., Flerchinger, G.N., 2010. Comparison of algorithms and parameterisations for infiltration into organic-covered permafrost soils. *Hydrol. Earth Syst. Sci.* 14, 729–750.
- Zoltai, S.C., 1993. Cyclic development of permafrost in the peatlands of northwestern Alberta. *Arct. Alp. Res.* 25, 240–246.